Chapter 5
Biomineralization: Tooth Enamel Formation

Mayumi Iijima, Kazuo Onuma, and Toru Tsuji

Abstract Tooth enamel is composed of well-crystallized apatite that elongates in the c-axis direction with a highly organized orientation. How do these crystals form? It is still an unanswered question, despite enormous efforts made on answering it.

Chapter 5 briefly reviews the physicochemical studies on clarifying the mechanism of enamel apatite formation. These studies revealed that enamel apatite crystals are formed in a fluid with discrete inorganic and organic compositions. The activity of inorganic ions changes dynamically during the formation process under strict cellular control, and it provides an adequate driving force for nucleation and successive growth. These processes include a dynamic equilibrium of inorganic ions and a transition of unstable intermediates to more stable phases. The composition and solubility of the forming enamel crystals also change dynamically. Because of this complex situation, several formation mechanisms of enamel apatite crystals have been proposed, and researchers have yet to reach a consensus on the subject. Crystal formation takes place in a gel-like enamel matrix, composed of spherical aggregates of amelogenin molecules. Amelogenin is a major component of the enamel matrix and regulates crystal formation by cooperating with enameline (minor matrix protein) and inorganic fluid components. Once enamel formation is

M. Iijima (✉)
Asahi University School of Dentistry, Oral Functional Science and Rehabilitation, Dental Materials Science, 1851-1 Hozumi, Mizuho, Gifu, 501-0296, Japan
e-mail: iijima@dent.asahi-u.ac.jp

K. Onuma
National Institute of Advanced Industrial Science & Technology, Central 6, 1-1-1 Higashi, Tsukuba, Ibaraki, 305-8566, Japan
e-mail: k.onuma@aist.go.jp

T. Tsuji
Advanced Research Centers, Keio University, 3-14-1, Hiyoshi, Kohoku-ku, Yokohama, 223-8522, Japan
e-mail: toruts2002@yahoo.co.jp

X.Y. Liu (ed.), *Bioinspiration: From Nano to Micro Scales*, Biological and Medical Physics, Biomedical Engineering, DOI 10.1007/978-1-4614-5372-7_5,

initiated, these proteins are degraded into smaller fractions, change the interaction with forming crystals and inorganic ions, and are gradually removed from the matrix, providing space for enamel crystals to grow. The chapter ends with a discussion of unique hard tissues with unusual mineral phases in vertebrate and invertebrates.

Keywords Tooth enamel • Apatite • Octacalcium phosphate • Amorphous calcium phosphate • Amelogenin

5.1 Introduction

Tooth enamel, the hardest tissue found in animals, has extremely long crystals with high crystallinity in parallel alignment. How the crystals are formed has been a controversial issue since the 1960s. In this chapter, enamel crystals and their surrounding environment are overviewed, and work aimed at clarifying the mechanism of tooth enamel biomineralization is discussed.

Abbreviations used for apatite-type compounds are:

Calcium hydroxyapatite: H-Ap
Calcium chlorapatite: Cl-Ap
Calcium fluorapatite: F-Ap
Carbonate-containing calcium hydroxyapatite: CO_3-HAp
Fluoride-containing calcium hydroxyapatite: F-HAp
CO_3, F, Cl-containing calcium apatite: CO_3, F, Cl-Ap
Biological apatite and calcium hydroxyapatite containing impurity ions, vacancies, and structural water: HAP

5.2 Enamel Crystals and Surrounding Environment

5.2.1 Overview of Tooth Enamel and its Formation

Tooth enamel is a highly mineralized tissue, with a composition approximately 95% HAP. Enamel crystals have an extremely elongated morphology from the dentin-enamel junction (DEJ) to the tooth surface, and they align parallel to each other (Fig. 5.1). The crystallinity of enamel HAP is almost equivalent to that of mineral apatites. An apatite with properties comparable to those of enamel HAP has not been obtained in vitro under physiological conditions.

Tooth enamel is formed by ameloblasts, which secrete an enamel matrix composed of water, proteins, and inorganic components. After the first layer of dentin has formed, the ameloblasts enter their formative stage. Moving away from

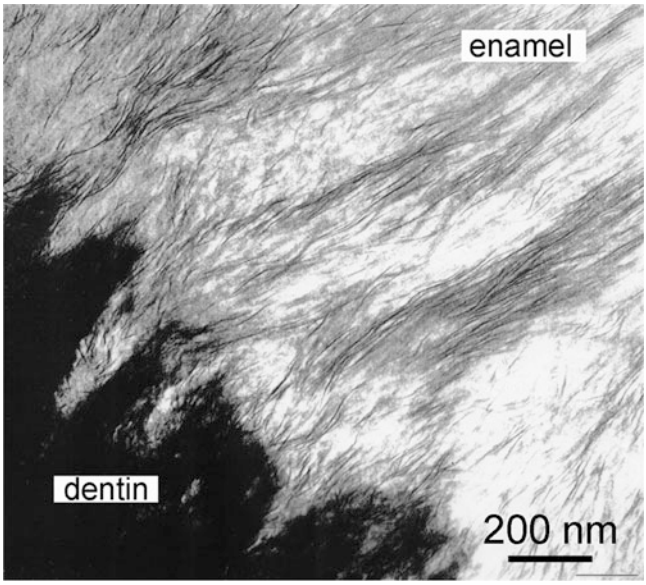

Fig. 5.1 TEM image of enamel in early stage of formation at dentin-enamel junction. In enamel, thin and ribbon-like crystals grow parallel to each other, while in dentin, tiny granules deposit in collagenous matrix. (Reproduced with permission from ref. [90]) (Copyright 1995, Springer)

the DEJ, they produce an enamel matrix in which enamel crystals grow. The enamel formation process is conventionally considered to occur in two stages [1]: organic matrix secretion and enamel crystal formation. In the first stage, enamel proteins secreted by ameloblasts form an enamel matrix [2], and the matrix partially mineralizes (to about 30% mineralization). In the second stage, the full thickness of the partially mineralized matrix is formed, and the degree of mineralization increases. The thickness of the enamel is specific to the animal species and tooth type. At a certain point in the secretory (first) stage, the matrix consists of 54% water, 31% proteins, and 15% mineral (by volume), with a density of 1.39 $g\,cm^{-3}$ [3]. In the maturation (second) stage, the enamel proteins are degraded by enzymes [4]. The degraded protein fractions and water are rapidly removed from the matrix by the ruffle-ended ameloblasts (RAs). At the same time, the RAs actively transport Ca^{2+} and PO_4^{3-} ions into the enamel matrix [5–10], enabling the crystal to increase in thickness. Thus, the water, organic, and mineral contents change during enamel formation [11, 12]. Mature human enamel contains about 1.8 wt% protein and has a density of about 2.9 $g\,cm^{-3}$[13]. Some proteins remain on the surface of the enamel crystals after most of the proteins have been removed from the matrix. As a result, the mineral content of the mature enamel is more than 95%. In contrast, degradation and removal of the structural matrix protein (collagen) does not occur in the mineralization of dentin and cementum.

5.2.2 Components and Characteristics of Enamel Matrix Proteins

The enamel matrix proteins consist of amelogenin, enamelin, sheathlin, and proteinases. Amelogenins account for about 90% of the enamel protein in the early stage of enamel formation. The 25 kDa amelogenins in porcine enamel matrix are cleaved almost immediately after being secreted and split into two fragments, a hydrophilic C-terminal region and a hydrophobic 20 kDa fragment, which is further cleaved into 13, 11, and 6 kDa fragments. The amino acid composition was initially characterized by enrichment in proline, glutamic acid, leucine, and histidine [14]. Since amelogenin has a highly aggregative property and multiple amelogenin genes, its characterization was a complicated puzzle [15]. The amino acid sequences of amelogenin were determined directly [16] or derived from the sequence of amelogenin cDNA [17]. It was a decade after the name "amelogenin" was bestowed by Eastoe [14]. After amelogenin was successfully expressed in an *Escherichia coli* system [18], investigation of amelogenin proceeded. The physicochemical properties are described in detail elsewhere, for example, solubility [19], aggregation [20–22], and interaction with HAP [23–25]. Proteomic and genetic of amelogenon are also studied [26–28]. The biology and physicochemical properties of amelogenin are reviewed by several authors [29, 30].

About 2% of the enamel protein is enamelin, which has a strong affinity for enamel crystal [31, 32]. It is also processed immediately following secretion producing intermediate fragments. Enamelin was isolated, purified, and characterized as an acidic glycoprotein enriched with aspartic acid, glutamic acid, serine, and glycine [33]. More detailed characterization then followed. Enamelin, like amelogenin, is processed immediately after secretion. Porcine intact enamelin (186 kDa) produces intermediate products (155, 145, 89, and 32 kDa) that are not stable, except the 32 kDa fragment [34–38].

The third minor component of the enamel matrix proteins is sheathlin, which has a distinctive amino acid composition, different from that of amelogenin and enamelin [39, 40]. Sheathlin distributes in the sheath (or interprismatic space) that partially separates the rod and inter-rod enamel [41].

The enamel matrix is characterized by two specific properties, which are mainly due to amelogenin: (1) the component changes during enamel formation as both amelogenin and enamelin degrade into several smaller fragments that are removed from the matrix; (2) the solubility, aggregation, and interaction with the mineral phase depend on the molecular weight, pH, temperature, and amelogenin and inorganic ion concentrations. Amelogenin and enamelin are now known to regulate enamel crystal formation.

5.2.3 *Enamel HAP Formation*

In the early stage of enamel formation, fine granules have been observed as an initial cell product [42, 43]. The process of thin ribbon-like crystallite formation from the granules comprises five main steps [42]: (1) deposition of granules (5–7 nm diameter) with low electron scattering; (2) linear assembly of granules into fibers (5–10 nm × 0.1–1.0 μm) with 5–7 nm periodicity and much greater electron scattering; (3) arrangement of fibers into parallel rows; (4) cross-linking of fibers by joining of electron-dense granules, resulting in a ladder-like appearance; and (5) deposition of many tiny crystallites, leading to the formation of ribbon-like crystals. Except for the initial granules with low electron scattering, all the electron-dense materials exhibit an apatitic electron diffraction pattern. This postulated process is related to the HAP formation mechanisms described by Beniash *et al*. [44]. Briefly, they observed that ACP particles form initially and that they assemble step-by-step into thin plates and eventually transform into HAP crystallites. They propose that the enamel proteins control the organized assemble of ACP particles and that the transition starts with proper ionic alignments within the ACP, which could dictate the direction of assembly. For details, see Chap. 4.6. Other candidates suggested as the initial enamel mineral phases are octacalcium phosphate (OCP) [45, 46], non-apatitic calcium phosphate [47], and ACP [48].

The ribbon-like enamel crystals align with their c-axes parallel to each other [49–51] (Fig. 5.1). The thickness was measured to be larger than 2 nm with distribution maxima at 2.5, 3, and 3.7 nm (newborn cat and 5-month-old human fetuses) [52]. The crystal length, obtained from enamel with a density less than 1.8 g cm^{-3}, is at least 100 μm, and the crystals are probably continuous from the DEJ to Tomes' processes [53]. In the maturation stage, the crystals increase mainly in thickness. As they do, they form plates characterized by flattened hexagonal cross-sections (Fig. 5.4c2). The thickening continues until the lateral faces of the crystals fuse to each other. Mature human enamel crystal has a mean width of 68 nm and a mean thickness of 26 nm [54]. Some researchers consider that the crystal length reaches, at most, the thickness of the enamel matrix [1].

5.2.4 *Microstructure of Enamel Matrix and Conformation of Amelogenin*

The morphological entities of the enamel matrix in the early formation stage have been variously described as fibrillar, compartmental or tubule, helical, and lamellar. These are reviewed by Nylen [55]. It is now generally accepted that amelogenin molecules assemble into spheres of nanometer size, which were initially identified as spherules with 15–20 nm diameter [20, 21], and that these nanospheres are the basic structural units of the enamel matrix (Fig. 5.2a). Further studies have shown that (1) the $–NH_2$ and –COOH groups [56] and hydrophobic regions [57] of the

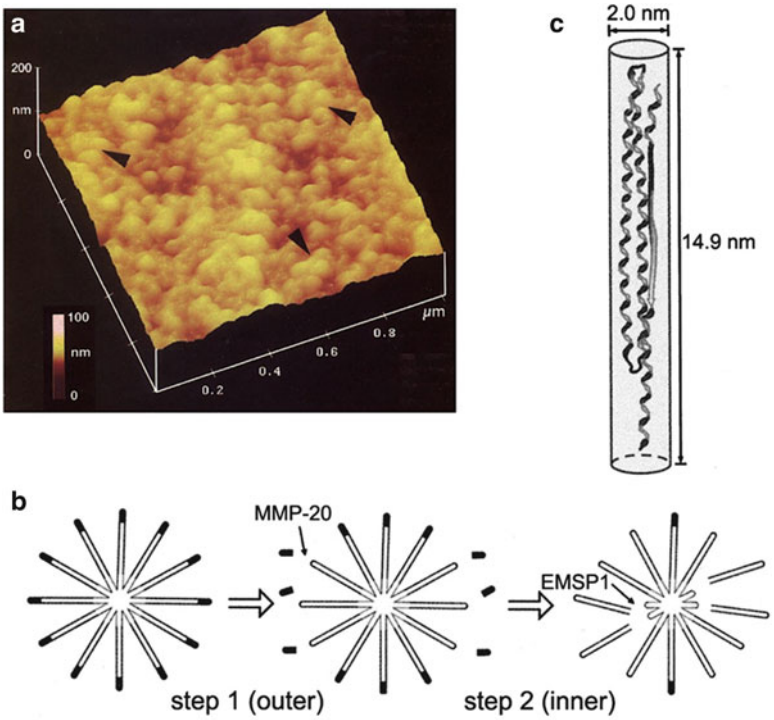

Fig. 5.2 (**a**) AFM image of porcine amelogenin gel (25 kDa (7.4%), 23 kDa (10.7%), and 20 kDa (49.6%) amelogenins and smaller peptides (32.4%)) formed at 4°C. Amelogenins assemble into nanospherules 8–20 nm in diameter. (Reproduced with permission from ref. [58]) (Copyright 1999, Elsevier) (**b**) Micelle model of 25 kDa amelogenin aggregate and proposed degradation by two-step cleavage that provides space for crystal growth: (step 1) hydrophilic C-terminal domain is cleaved by protease MMP-20; (step 2) cleavage by protease EMSP-1 releases 13 kDa fragments, leaving behind smaller micelles containing 6 kDa fragments. (Reproduced with permission from ref. [64]) (Copyright 2007, Sage Publication) (c) Model structure of amelogenin molecule (porcine, 20 kDa fragments) with three characteristic domains: β-sheet, polyproline, and random coil. (Reproduced with permission from ref. [77]) (Copyright 2009, Wakaba Publishing Inc.)

amelogenin distribute outer surface of the nanospheres; (2) the nanospheres vary in size depending on the molecular weight of the amelogenin and the pH, temperature, and protein concentration of the solution [22, 58, 59]; and (3) the nanospheres tend to form chains, which assemble into higher order structures, "microribbon," in vitro [60]. Structure of amelogenin is reviewed by several authors [61–63], and also described in 2.2 of Chap. 4.

Another model structure based on the behavior of amelogenin in solution has been proposed (Fig. 5.2b) [64]. In this micelle model, the surfaces of the 25 kDa amelogenin micelles have a highly hydrophilic C-terminal domain, which has a pattern of positive and negative charges. The micelles aggregate by ionic interaction. Micelles of 20 kDa amelogenin without the C-terminus aggregate

through hydrophobic bonds. The size of the micelles decreases as the C-terminal and 13 kDa regions are sequentially cleaved by MMP-20 [65] and EMSP-1 [66] (step 1 and step 2, respectively; Fig. 5.2b). The C-terminal and 13 kDa regions are removed from the micelles, leaving behind smaller micelles comprised of 6 kDa fragments. This provides growth space for enamel crystal.

The conformation of amelogenin molecules in solution was determined using circular dichroism (CD) and small-angle X-ray scattering (SAXS). These studies revealed that amelogenin molecules, which consist of some 180 amino acid residues, do not behave like a globular protein in solution. Porcine amelogenin molecules (20 kDa) consist of discrete folding units in the N-terminal, central, and C-terminal regions and have a β-sheet structure, a polyproline structure, and a random coil structure, respectively [67]. In 0.1–0.3 μg protein/ml 2% (v/v) acetic acid solution (pH5.3, 25°C), 20 kDa amelogenin forms an elongated bundle structure and assumes a monomeric form [67], while in 10 μg protein/mL 2% (v/v) acetic acid solution (pH < 5.3, 5°C), 20 kDa amelogenin (length of 15 nm and diameter of 2 nm) (Fig. 5.2c) assumes a dimmer form and exhibits an overall radius of gyration of 4.4 nm [68]. When rodlike molecules with both hydrophobic and hydrophilic terminals aggregate, formation of a micelle structure cannot be ruled out.

5.2.5 Ionic Composition and pH of Enamel Fluid

Separation of the enamel fluid from the secretory stage of the matrix enabled the ionic composition to be measured and the degree of saturation of the enamel fluid to be calculated with respect to the enamel HAP and related calcium phosphate [69, 70]. The water content in the secretory stage was around 30–40% of the wet weight [12]. The average composition of the enamel fluid during the secretory stage was total [Ca^{2+}] 0.5 mM, total [P] 3.9 mM, [Mg^{2+}] 0.8 mM, [Na^{+}] 140 mM, [K^{+}] 20 mM, [Cl^{-}] 150 mM, [F^{-}] 5×10^{-3} mM, and total [HCO_3^{-}] 9.74 mM. The pH, the ionic strength, and the osmolarity were 7.26, 165 mM, and 312 mosmol/kg H_2O, respectively. The pH was measured under a constant CO_2 partial pressure. The concentration of free Ca^{2+} ions (0.15 mM) was about 30% of the total Ca^{2+} concentration; the remaining 70% were bound with other inorganic ions and proteins. The total concentration of Ca^{2+} was about half that in the predentin (1.0 mM) and in the fluid of enamel organ tissue surrounding the developing teeth (1.3 mM) and was much lower than that in the blood plasma (2.5 mM). On the other hand, the PO_4^{3-}concentration of the enamel fluid (3.5 mM) was about three times that in the blood plasma (1.1 mM). The activity of Ca^{2+}, (a_{Ca}), calculated taking into account the thermodynamic factors, was 0.053 mM. The calculated free HCO_3^{-} concentration in enamel fluid was around 10 mM, lower than that of the blood plasma CO_3^{2-} concentration (about 22 mM). The calculated degree of supersaturation with respect to H-Ap, OCP, and enamel HAP suggests that the enamel fluid was supersaturated with H-Ap, undersaturated with OCP, undersaturated with enamel HAP at a pH lower than 7.1, and supersaturated with

enamel HAP at a pH higher than 7.1. Thus, the compositions of the enamel fluid and enamel crystal change during enamel formation. Direct staining of developing bovine enamel with pH indicators demonstrated that the enamel matrix has alternate acidic (pH5.8–6.0) and neutral (pH7.0–7.2) areas [71] at certain locations and times during enamel HAP formation.

During enamel HAP formation, Ca^{2+} ions are actively transported from the ameloblasts into the enamel matrix, and the amount and timing of the Ca^{2+} inflow are strictly controlled by the ameloblasts (2.2). The inflow of the Ca^{2+} increases rapidly during the maturation stage [10]. This could increase the total Ca^{2+} concentration in the matrix. However, the a_{Ca} is decreased due to the chemical equilibrium of the ionic components in the enamel fluid. These components include lactate, $H_2PO_4^-$, HPO_4^{2-}, PO_4^{3-}, HCO_3^-, and CO_3^{2-}.

The a_{Ca} is also controlled by the surrounding amelogenins. The 25 kDa amelogenins are cleaved by enzymes step-by-step during enamel formation, forming 20, 13, 11, and 6 kDa fragments. The cleaved fragments show different binding abilities with Ca^{2+} and the developing crystal. The concentration of 13 and 11 kDa fragments is 2.8 w/v% in the secretory stage of porcine enamel matrix [23]. This corresponds to a 2 mM protein concentration when calculated using a molecular weight of 13 kDa. This is several times higher than the concentration of Ca^{2+} in the enamel fluid (0.3–0.5 mM). The binding coefficient of the proteins and Ca^{2+} ions is of the order of 10^4 M [72], strongly suggesting that the fragments work as a Ca^{2+} reserve.

5.3 Mineral Component of Tooth Enamel

5.3.1 Composition and Solubility of Enamel HAP

Enamel HAP contains several impurity ions, vacancies, and structural water [73]. The chemical composition solubility of porcine enamel in the early and late secretory stage and maturation stage has been determined [74, 75]. The chemical formula for the thin ribbon-like crystals in the early stage of maturation is $(Ca)_{4.155}(Mg)_{0.034}(Na)_{0.191}(K)_{0.004}(HPO_4)_{0.35}(CO_3)_{0.357}(PO_4)_{2.384}(OH)_{0\cdot007}$.

That for erupted mature enamel is $(Ca)_{4.568}(Mg)_{0.032}(Na)_{0.11}(K)_{0.002}(HPO_4)_{0.143}(CO_3)_{0.256}(PO_4)_{2.712}(OH)_{0.378}$.

The relatively large decrease in HPO_4 during enamel formation is ascribed to the OCP-to-HAP phase transition [76]. The amount of Mg^{2+} substituted for the Ca^{2+} is almost constant, 0.7–0.8% of the Ca^{2+}, among developing enamel crystals.

The solubility products (K_{sp}) of developing enamel crystals at different stages were determined on the basis of the chemical composition $(Ca)_{5-x}(Mg)_q(Na)_u(HPO_4)_v(CO_3)_w(PO_4)_{3-y}(OH)_{1-z}$. The average ion activity product $(I_{APeq})^{1/N}$ (N is the sum of the valences for each ion comprising the solid phase; for details, see 1.3.1) had a level of 4.41×10^{-6} in the early secretory stage, 1.80×10^{-6} in the

early maturation stage, and 1.45×10^{-6} in erupted enamel [77]. Thus, the solubility of the enamel crystals decreases as maturation proceeds; in other words, the stability of enamel crystals increases with maturation.

The solubility of F-HAp with different F^- contents is minimum (6.55×10^{-63}) when almost half the OH^- has been replaced with F^- ($Ca_5(PO_4)_3(OH)_{0.43}F_{0.57}$) [78]. The relationship between the F^- content in enamel and HAP stability gives important information about the formation and prevention of caries and the remineralization of tooth enamel. Much information about the composition of apatites and their properties is readily available (for example, [79–81]).

5.3.2 CO_3-HAp and Properties of CO_3^{2-} in CO_3-HAp

The mineral component of mammalian tooth enamel is generally described as CO_3-HAp. The CO_3^{2-} is an important lattice component because it regulates the solubility, morphology, and size of biological HAP [82, 83]. Whether CO_3^{2-} can replace OH^- in the HAP lattice was a controversial issue because of the geometric restrictions caused by the form and size of PO_4^{3-} (regular tetrahedron), CO_3^{2-} (equilateral triangles), and OH^- (linear). Strict analysis of CO_3-HAp ($Ca_{10}(PO_4)_{5.99}(CO_3)_{0.86}(PO_4)_{2.384}(OH)_{0.26}O_{0.02}$) showed that one CO_3^{2-} replaces two OH^- and the plane of CO_3^{2-} triangles is almost parallel to the *c*-axis [81]. This parallel orientation creates much less steric interference than the perpendicular orientation. When CO_3^{2-} has replaced OH^-, it is defined as A-type CO_3; when it has replaced PO_4^{3-}, it is B-type CO_3; and when it has replaced OH^- and PO_4^{3-}, it is AB-type CO_3.

In developing enamel HAP, not only the CO_3^{2-} content, but also the ratio of the replacement sites, i.e., PO_4^{3-} or OH^-, changes during maturation [74]. In young and immature enamel HAP, substitution for PO_4^{3-} is favored, and then, as maturation progresses, substitution for OH^- is increasingly favored. Incorporation of CO_3^{2-} in HAP increases with an increase in the CO_3^{2-} concentration of the surrounding fluid, and substitution for PO_4^{3-} is favored under neutral pH conditions [84]. Such diversity in substitution and site occupancy of CO_3^{2-} in enamel crystal has been ascribed to changes in the enamel fluid composition and the pH conditions during the formation process.

5.3.3 Crystal Structure of HAP

The crystal structure of synthesized H-Ap was described initially as an F-Ap type, e.g., hexagonal, $P6_3/m$, with the O of the OH^- at (0,0,0.25) [85]. Later analysis using mineral H-Ap (Holly Spring, United States) by both X-ray and neutron diffraction technique [86] showed that the O is at (0,0,0.201) and that the H is at

(0,0,0.062). Because the OH^- is slightly displaced from the mirror plane ($z = 0.25$ and 0.75), the stability of H-Ap is slightly lower than that of F-Ap [87]. The crystal structure of human enamel was determined using the powdered enamel fraction with a density higher than 2.95 g cm^{-3} and the Rietveld method [88]. Enamel HAP has almost the same structure as H-Ap and structural water, and Cl^- (about 0.3 wt%) is located on the hexagonal axis between $z = 0.11$ and 0.14. Structural water is defined as water in the lattice that is removed by heating at 400°C. The lattice dimensions are $a = 0.9441(2)$ and $c = 0.6878(1)$ nm. The loss of water from enamel HAP decreases the a-axial dimension by 0.02 nm [89]. Structural aspects of HAP are also described in Chap. 3.2.

As described in Chap. 3.2, H-Ap has two possible symmetries, hexagonal and monoclinic. It has been noted that a small number of impurity ions, e.g., F^-, stabilizes the hexagonal structure [90]. Therefore, strictly speaking, any HAP, including enamel HAP, that contains impurity ions is not genuinely hexagonal but pseudohexagonal with its hexagonal symmetry stabilized by the ions.

5.4 Mechanisms of Enamel Crystal Formation

5.4.1 Regulatory Roles of Amelogenin and Enamelin

How does enamel crystal formation start? Dentin at the DEJ was once thought to be the nucleation site on the basis of transmission electron microscopy (TEM) observations of the dentin and enamel crystallites at the DEJ [91]. However, there is little other evidence supporting the nucleation of enamel crystal on dentin crystal at the DEJ. Direct epitaxial growth of enamel crystals onto dentin crystallites has not been observed [42, 92]. Along with ultrastructural studies of developing enamel crystals, in vitro HAP formation studies have shown that amelogenin accelerates the nucleation kinetics and controls the crystal morphology, indicating that the crystal formation mechanism involves amelogenin [93–96]. Nuclear magnetic resonance (NMR) studies showed that the C-terminus of amelogenin, with four $–COO^-$ groups and three $-NH^+$ groups, directly binds with the HAP crystal surface [97]. In vitro nucleation and growth of OCP are promoted by recombinant amelogenin (rP179) with the C-terminus [98]. Promotion of OCP nucleation is ascribed to the $–NH^+$ and $–COO^-$ groups in the charged C-terminal region exposed on the surface, which could reduce the nucleation energy. A role of rP179 in the OCP formation is also discussed in Chap. 4.4.

The adsorption behavior varies with the molecular weight [24]. Intact amelogenin (25 kDa for porcine) adsorbs strongly on HAP while the 20 kDa fragments adsorb less strongly [23]. The 13 kDa fragments adsorb less than the nascent 25 kDa amelogenin molecules. Ultrastructural studies of developing enamel crystals have shown that amelogenin nanospheres are on and between the developing enamel crystals [61]. Chemical force microscopy observations [99] demonstrated

that amelogenin nanospheres preferentially bind to positively charged domains of enamel crystal. Thus, functional control of crystal size, morphology, orientation, and growth rate has been ascribed to amelogenin.

Since enamelin has a strong affinity for enamel crystal (2.2), it is considered to induce nucleation and to regulate the growth rate through interaction with the crystal. The 32 kDa fragment, one of the series of cleavage products, is the most stable one. It has been shown to promote nucleation of apatite [100] and to change its conformation from α-helix to β-sheet, which interacts with Ca^{2+} in HAP, depending on the Ca^{2+} concentration [101].

Cooperative regulation of enamelin and amelogenin through their interaction has been suggested [102]. The hypothesis that amelogenin and enamelin jointly control the elongated crystal growth of OCP was examined [103] using a dual membrane experimental device in which a cation-selective membrane and a dialysis membrane form a tiny reaction chamber, and Ca^{2+} and PO_4^{3-} ions flow into the chamber in a controlled manner. OCP was chosen as a model crystal for the post-secretory growth on the basis of the evidence described in 4.6 and 4.7. A mixture of 10w/v% recombinant porcine amelogenin (rP148) and 32 kDa porcine enamelin fragments was used as a crystal growth medium at 37°C and a pH of 6.5. The aspect ratio of the OCP crystals was substantially higher at a certain ratio of amelogenin to enamelin. Thus, the co-assembly of amelogenin and 32 kDa enamelin was suggested as a mechanism regulating the morphology of OCP crystal.

5.4.2 ACP Formation and Stability in Enamel Fluid

As described in Chap. 3.2, there is no general agreement yet on the solubility product of ACP, which is required to evaluate the driving force ($\Delta\mu$) needed to precipitate ACP. Several solubility products, ranging from 24.8 to 28.3, have been proposed for ACP and amorphous tricalcium phosphate (ATCP). ACP slurry (for which a large solid/solution ratio is the best experimental approach) has a nearly constant I_{AP} of 1.6×10^{-25} in the pH range 7.4–9.25 when the formula is given as $Ca_3(PO_4)_{1.87}(HPO_4)_{0.2}$ [104]. Accordingly, "the minimum I_{AP} needed to form ACP de novo in physiological solution at pH7.4 is considerably greater than that calculated for serum" [105]. In general, the spontaneous formation of ACP is attained by mixing Ca^{2+} and PO_4^{3-} solutions with rather high concentrations of Ca^{2+} and PO_4^{3-}. The Ca^{2+} and PO_4^{3-} immediately co-aggregate into clusters large enough to be separated from the solution. However, the Ca^{2+} and PO_4^{3-} concentrations of the enamel fluid are too low to form ACP spontaneously (2.5, 3.1). Therefore, "it would appear unlikely that ACP could form in vivo" [105] without a mechanism to increase the local Ca^{2+} and PO_4^{3-} concentrations or a reasonable process to form nuclei. As described in 4.4, the mechanism could be the stepwise construction of growth units by amelogenin and pre-nucleated CaP clusters.

Although ACP is not very stable and transforms into crystalline phase in pure calcium phosphate solution, in vitro studies have shown that CO_3^{2-}, Mg^{2+}, F^-,

and $P_2O_7^{4-}$ stabilize ACP [83, 106, 107]. The potential role of a PO_4^{3-} group of amelogenin in ACP stabilization was demonstrated: P148 with a PO_4^{3-} group on serine-16 stabilized ACP for more than one day while non-phosphorylated rP172 did not [108]. ACP, once formed, could be stabilized in the enamel matrix for some period.

5.4.3 Organization of ACP into Crystals

Supramolecules composed of amelogenin and ACP have been formed in vitro [51]. The unanswered question is, "what controls the arrangement and fusion of the supramolecules and transformation into crystallines with their c-axes parallel to each other?" Since there are charged domains on developing enamel crystal surfaces [99], the domain structure of the enamel crystals is thought to be formed by the organized fusion of the crystallites in the c-axis direction. HAP crystal formation by stepwise fusion of the protein/mineral nanoparticles into long crystals was proposed [109]: initially formed fine granules align in rows and form chains by fusion; the chains fuse into plates, and the plates fuse along the c-axis direction, forming long crystals.

In the absence of a structural framework or functional materials, it would be hard to control the assembly of ACP and the final morphology of the crystalline phase derived from ACP. ACP particles formed in solution frequently aggregate into irregularly shaped branching clusters, and de novo crystallization yields crystals with a rectilinear morphology [105]. Since a spherical-shaped ACP particle has no long-range order in its structure, there must be mechanisms that organize the assembly of ACP particles and their successive growth into crystals with morphology specific to the hard tissue. Beniash *et al*. noted that partially ordered structure formed in ACP particle could dictate the direction of assembly [44].

5.4.4 CaP-Cluster Models

The formation models postulated by Wang *et al*. and Yang *et al*. ascribe this function to amelogenin and explain the process specifically [95, 96]. Both of them studied the effect of amelogenin (rP172) on nucleation and growth of HAP under strict control of the degree of supersaturation with respect to the precipitating phases using a constant composition technique [110].

Wang *et al.* used solutions supersaturated with respect to OCP ($\sigma_{OCP} = 1.45$ and 2.32) with pH 6.8 and 37°C to examine whether enamel HAP forms with OCP as an intermediate phase [95]. Figure 5.3 illustrates the step-by-step mechanism of the assembly of CaP clusters and amelogenin nanospheres into HAP crystal. In the presence of amelogenin, the induction time is less. Nucleation clusters

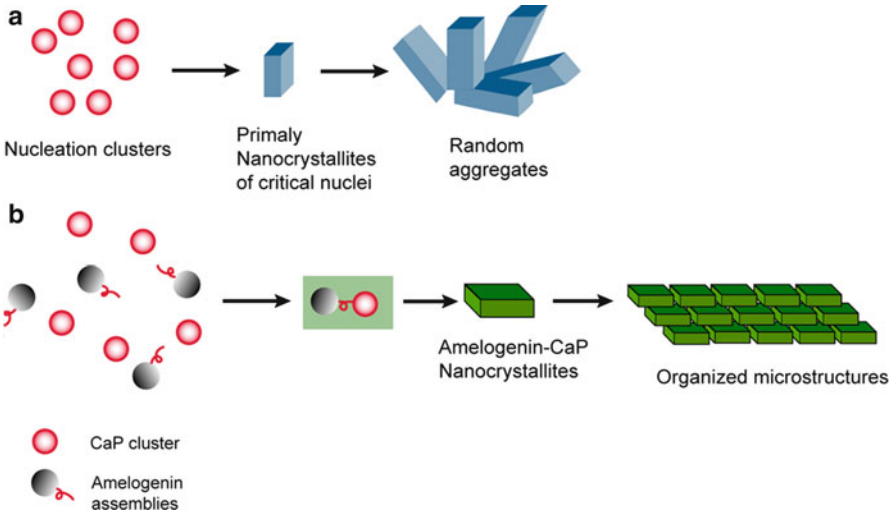

Fig. 5.3 Model of crystal formation in solution supersaturated with OCP: (a) without amelogenin, random aggregates of OCP form. (b) With amelogenin, organized microstructures form: (1) assembly of CaP clusters (red balls) and amelogenin oligomers (small nanospheres, gray ball); (2) formation of amelogenin-CaP nanocrystallites as building units; (3) organized assembly of building units into HAP nanocrystallites. (Reproduced with permission from ref. [95]) (Copyright 2007, American Chemical Society)

(CaP clusters) bind with amelogenin nanospheres and form amelogenin (amel)-CaP clusters as basic building units. These clusters form amel-CaP nanocrystallites, which subsequently assemble and form HAP nanocrystallites. The specific binding is ascribed to the charged COOH-terminal region. An important point is that amel-CaP nanocrystallites find the low-energy configurations needed to bind with the adjacent crystallite. An NMR study revealed a direct amelogenin-HAP interaction through the C-terminal region that oriented the C-terminal region on the HAP crystal [97]. Without amelogenin, spherical aggregates of OCP nanocrystallite formed.

Yang *et al*. used a solution with H-Ap stoichiometry and undersaturated with respect to OCP to analyze the nucleation process: $\sigma_{HAP} = 15.1$, pH 7.4, 37 °C, ionic strength = 0.15 M, with rP172 of 25 μg/mL [96]. The reactions in solution with lower supersaturation revealed the initial nucleation process. The newly observed crystal formation process comprises five steps: (1) CaP clusters pre-nucleate with a diameter of less than 1 nm. (2) The pre-nucleated clusters are captured by amelogenin, causing them to form amel-nano-CaP clusters, 2–10 nm in size, which in turn form nanoparticles, 30–50 nm in size. The amel-CaP nanocluster composites transform into amel-ACP nanospherical building blocks. (3) The amel-ACP nanospherules gradually assemble into nanochains. (4) The nanochains co-assemble into nanorods or nanoribbons. (5) Ostwald ripening leads to elongated HAP.

Without amelogenin, random-sized CaP clusters formed and assembled into globular ACP with an irregular size distribution. This globular ACP aggregated

and partially transformed into crystalline HAP although remaining ACP in the final product. In this process, the induction time is reduced by the amelogenin, indicating that amelogenin promotes the formation of pre-nucleated CaP and amel-CaP clusters. The postulated roles of amelogenin are (1) capturing and stabilizing the pre-nucleated CaP clusters, (2) controlling the aggregation of primary-composite nanoclusters into the initial building blocks, and (3) controlling the sequential assembly of the building blocks in the post-nucleation crystal growth stage.

Thus, the size of the initial CaP clusters and the growth unit are determined at the atomic level by amelogenin and the solution conditions. The spherules formed in the Ca-PO_4 solution with rP172 were mainly 0.8–1.4 nm, while the rP172 spherules were larger than 10 nm. This strongly suggests that the initially formed phase is CaP clusters (pre-nucleated), which are stabilized by rP172 [108], enabling them to serve as building blocks for the nanocluster composites. Note that the size of 0.8–1.4 nm is comparable to a hydrodynamic radius of aggregates (about 0.5 nm) detected in pseudo-body fluid [111, 112] (see 3.4.7 in Chap. 3).

5.4.5 Transformation from ACP to HAP and Intermediate OCP

The phase transformation from ACP to HAP was extensively investigated by thermodynamic analysis in the 1970s [113–115]. These studies postulated that the transition involves OCP and the transition usually starts before all the ACP has transformed into OCP because OCP is a very unstable intermediate of H-Ap. The lifetime of OCP is remarkably reduced in the presence of a small amount of F^-, in a basic solution, and at a higher Ca/PO_4 molar ratio. This makes it difficult to detect the intermediate phase. Therefore, OCP has been recognized as a labile intermediate. However, even when OCP was not detected as an identifiable solid phase, solution chemistry has shown that when OCP is forming in solution, the I_{AP} of the solution is larger than the solubility product of OCP [115]. This is thermodynamic evidence for the existence of OCP. For detail in this area, review is available [116].

In the transformation from ACP to HAP, OCP is usually observed as the first crystal in close contact with the surfaces of ACP particles [117, 118]. The subsequent transformation from OCP to H-Ap appears to be in situ, whereby the OCP undergoes a solid-state rearrangement into an H-Ap structure [45]. The first crystalline phase detected usually gives an apatitic X-ray diffraction (XRD) pattern with the a-axial dimension larger than that of HAP. This indicates that there is an OCP-like structure in the crystal [119]. For the transformation from ACP to H-Ap, review is available [105].

5.4.6 Possibility of OCP Involvement in Enamel HAP Formation

In the mechanisms of extremely long and well-crystallized enamel crystal formation, Brown *et al.* recognized the importance of OCP and theorized that OCP is a precursor of enamel HAP [45, 119]. They considered it to be a precursor because (1) OCP has a thin and platy morphology, while HAP has a hexagonal one; (2) OCP grows more rapidly than HAP; (3) OCP is a metastable phase of HAP; (4) unstable OCP readily transforms into stable-phase HAP, and (5) OCP is structurally similar to HAP. HAP formation via OCP occurs in three stages: (1) nucleus formation, (2) two-dimensional growth of OCP into a single unit-cell thickness of OCP, and (3) precipitation of a unit-cell thickness of OCP on the two-dimensional crystal and its hydrolysis. Since the transformation from OCP to HAP is topotaxial, the crystallographic axes of the OCP are preserved after the transformation. The phase transformation from OCP to HAP has been proposed as the mechanism incorporating impurity ions, water, and vacancies into HAP [119]. Although many HRTEM studies of enamel in the early formation stage caught images of OCP in the first-formed enamel crystals [52, 120–122], Brown *et al.*'s OCP precursor theory has not been generally accepted due to the difficulty of detecting a transient mineral phase.

HPO_4^{2-} is another indicator that supports the involvement of the acidic precursor phase [79, 123]. As described in 3.1, HPO_4^{2-} is a substantial lattice component of developing enamel crystals. Fourier transform infrared spectroscopy (FTIR) studies have shown that the HPO_4^{2-} group is a lattice component of the enamel crystals [74]. The amount of HPO_4^{2-} decreases with the progress of crystal maturation [76]. The higher content of HPO_4^{2-} in the early secretory enamel is consistent with the formation of an OCP-like phase.

Micro-Raman spectroscopy, which is very sensitive to the atomic order of the phase, revealed the presence of OCP in living murine calvarial tissue [124]. This was the first direct evidence without the artifact of dehydration. Moreover, there was an indication that ACP may form prior to OCP. Thus, in the case of murine calvarial tissue, bone HAP formation could include the transition of ACP to OCP.

5.4.7 Epitaxial Overgrowth of Apatite on OCP Template

CO_3-HAp crystals with central planar defects were synthesized for the first time by Nelson *et al*. (Fig. 5.4a1) [125]. The cross-sectional HRTEM images of the crystals resemble those of enamel HAP crystals with a central dark line (CDL) [50, 126, 127]. Fourier filtering analysis of lattice images of the CO_3-HAp crystals showed that the defects were a one- or two-unit cell thickness of two-dimensional OCP (Fig. 5.4a2) [128]. The two-dimensional OCP was parallel to the (100) plane of the CO_3-HAp. A growth model, epitaxial overgrowth of apatite on the OCP template,

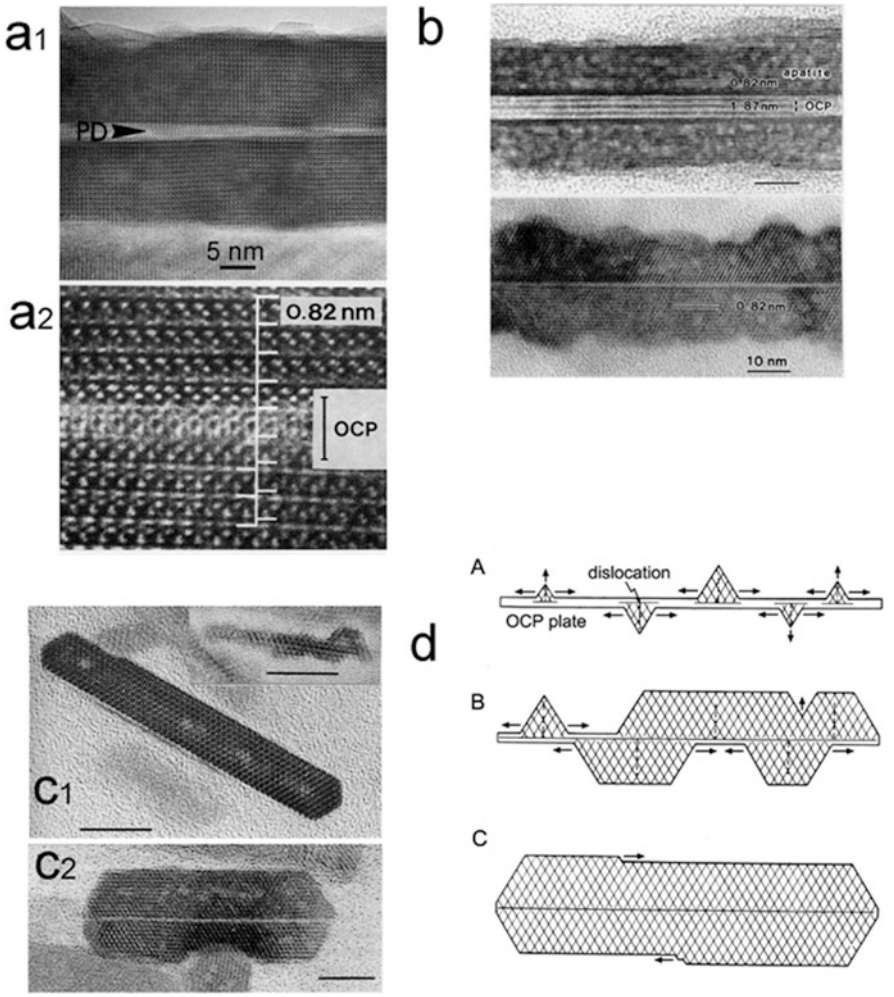

Fig. 5.4 (a1) Cross-sectional lattice image of synthesized CO_3-HAp crystal with central planar defect; (a2) higher magnification image of defect region. Central, one-unit-cell-thick OCP region is labeled; white markings show expansion of apatite lattice across defect. (Reproduced with permission from ref. [128]) (Copyright 1989, John Wiley and Sons) (b) Ap/OCP/Ap lamellar mixed crystals grown on a cation-selective membrane in the presence of 1 ppm F. (Reproduced with permission from ref. [135]) (Copyright 2001, S. Karger AG) (c1) Puffer enamel crystals in early overgrowth stage. (Reproduced with permission from ref. [130]) (Copyright 1991, Springer) (c2) Carp enameloid crystal in maturation stage. (Reproduced with permission from ref. [131]) (Copyright 1991, Springer) Horizontal bar corresponds to 10 nm. (d) Model of lateral epitaxial overgrowth of enamel crystals: (A) epitaxial growth of apatite on OCP template with one-unit-cell thickness; (B) lateral growth of isolated apatite units on template and fusion of neighboring units; (C) thickening of apatite crystals by acquisition of apatite unit cells on their prism plane. (Reproduced with permission from ref. [120]) (Copyright 1993, Springer)

was postulated to explain the central planar inclusion. Briefly, a primordial thin plate of OCP crystal works as a template for successive epitaxial growth of HAP on the (100) face, with the template embedded at the center of the HAP crystal. This model well explains the formation mechanism of the CDL, which is observed in the cross-section of enamel HAP.

A series of Ap/OCP/Ap lamella mixed crystals ([129a]) (Fig. 5.4b), developing porcine enamel crystals [120], puffer enamel HAP [130] (Fig. 5.4c1), and carp enameloid HAP [131] (Fig. 5.4c2) ensure HAP overgrowth on an OCP template in vivo and in vitro. In the Ap/OCP/Ap mixed crystals, the thickness of the OCP at the center decreased while that of the apatite overgrowth increased with an increase in the concentration of F^- from 0.1 to 1 ppm. In the presence of 1 ppm F^-, HAP with a central planar defect was obtained; cross-sectional HRTEM images of these Ap/OCP/Ap lamella mixed crystals (Fig. 5.4b) were similar to those of Nelson's CO_3-HAp crystal, carp enameloid crystals [131] and of porcine enamel crystals [120]. TEM observation has shown that the OCP template grew to its critical size, and then HAP overgrowth on the template crystal commenced [129b]. The critical size of the template depended on the solution conditions (pH, ion concentration, etc.). Interestingly, crystals with the Ap/OCP/Ap structure have been found in human dental calculus [132].

On the basis of HRTEM observation of developing fish enameloid, porcine enamel HAP, and synthesized CO_3-HAp crystals, the epitaxial overgrowth mechanism was modeled at the atomic level [120] (Fig. 5.4d): (1) two-dimensional growth of an OCP-like precursor with a one- or two-unit cell thickness and a ribbon-like morphology; (2) epitaxial overgrowth of apatite on the thin ribbon in which small, regular triangles and trapezoid crystals form as building units and are deposited on screw dislocations of the precursor crystal; (3) lateral growth of the small triangles on the template and fusion of the neighboring units; and (4) thickening of the template crystal by two-dimensional growth on the prism plane. Screw dislocations, which initiate HAP overgrowth, have been observed in both synthetic CO_3-HAp [125] and human fetal enamel crystals [127].

5.4.8 Control of Morphology and Orientation by One-Directional Ca^{2+} Diffusion

The ameloblasts secrete enamel precursor materials in the direction of their long axis. Osborn suggested that the crystal orientation is controlled by the secretory force generated by the ameloblasts [133]. This suggestion led to the supposition that one-directional Ca^{2+} ion supply from the ameloblasts causes the lengthwise and oriented growth during the initial crystalline phase, which was assumed to be OCP [134]. A model system constructed for this uses a cation-selective membrane to create one-directional diffusion of Ca^{2+} ions, thereby simulating the flow of Ca^{2+} ions in the enamel matrix. OCP crystals elongated in the c-axis direction grow on the membrane with the c-axes parallel to each other. Details are reviewed by Iijima [135].

The formation of OCP usually starts with deposition of granules about 100 nm in size on a membrane [136]. These granules do not show any distinctive XRD reflection, suggesting that they are ACP-like precipitates. They deposit on the membrane and assemble into irregularly shaped branching clusters, which subsequently grow into bank-like structures and then flake-like crystals. The flake-like crystals increase in height perpendicular to the membrane and eventually grow into OCP crystals elongated in the *c*-axis direction. The transition from amorphous to crystalline phase is speculated to be a de novo rearrangement of the internal structures.

5.4.9 *Correlated Interaction of F^-, Amelogenin, and Ca^{2+} in HAP Growth*

The effects of F^- on the formation and properties of HAP crystals are well known. F^- (1) increases the growth rate, (2) accelerates the hydrolysis of OCP to HAP, (3) improves the crystallinity, (4) increases the crystal size, and (5) reduces the solubility. In the combination of F^- and amelogenin, the F^- induces and precedes F-HAp formation, and the amelogenin disturbs this reaction. Amelogenin adsorption on the F-HAp crystals increases with the F^- content. F-HAp adsorbs more amelogenin than H-Ap. Since the F^- in F-HAp interferes with protease activity, the amelogenin on crystals is less degradable, so it is retained on the F-HAp longer [137].

In addition, Ca^{2+} is related to the adsorption of amelogenin on the crystals. The higher the Ca^{2+} concentration, the more rapidly the amelogenin is degraded and removed from the crystal. A higher Ca^{2+} concentration also promotes F-mediated conversion of OCP to HAP in vitro [137]. In the secretory stage, when Ca^{2+} transport is limited, degradation of amelogenin progresses slowly, while early in the maturation stage, when Ca^{2+} transport increases dramatically, the transition from OCP to HAP, the degradation of amelogenin, and the removal of the degraded fractions are accelerated. The removal of the fractions enables the F^- to adsorb on the crystal, leading to formation of F-HAp. Since F-HAp enhances amelogenin adsorption, there is an amelogenin reaction that disturbs crystal growth. Thus, F^-, Ca^{2+}, and amelogenin interact with enamel HAP in a coordinated manner.

5.4.10 *Regulation of OCP and HAP Formation by Amelogenin and F^-*

Considering OCP to be another transient phase for enamel crystals, Iijima *et al*. investigated the growth mechanism of elongated OCP crystals using a dual membrane experimental device [138–140]. OCP crystals preferentially grew in the c-axis direction on the membrane regardless of the presence of amelogenin. Amelogenin decreased the OCP crystal size. The degree of decrease was in the

order width < length < thickness. In other words, the degree of interaction of amelogenin with the OCP crystal faces was in the order (010) > (001) > (100), meaning that the interaction with the (010) face was the strongest. Thus, the aspect ratio was increased by preferential interaction of the amelogenin with the side faces of the OCP crystals. This was observed regardless of the presence of the hydrophilic C-terminus and the type of amelogenin used. Therefore, the interaction between OCP and amelogenin was ascribed to the hydrophobic core part of amelogenin. Fluoride (1 ppm) changed the mineral phase from OCP to HAP, yielding oriented prism-like HAP crystals with a large aspect ratio [139]. It is possible to incorporate F^- into the lattice to enhance the interaction between the amelogenin and crystal [137].

5.4.11 Cooperative Regulation of HAP Growth by Amelogenin, Ca^{2+}, and Mg^{2+}

Analysis of the adsorption of amelogenin, Ca^{2+}, and Mg^{2+} on growing enamel crystals [137] revealed that amelogenins adsorb on enamel crystals more preferentially than Mg^{2+}. In the maturation stage, as the proteolytic cleaving of amelogenin proceeds, amelogenin fragments are removed from the crystals while Mg^{2+} adsorption increases. Since Mg^{2+} adsorption is suppressed by amelogenins, the removal of amelogenin enables Mg^{2+} to adsorb. The adsorption ability of Mg^{2+} is about one-third that of Ca^{2+}, and the adsorption of Mg^{2+} decreases with the activity ratio $(a_{Mg})/(a_{Ca})$. This means that Ca^{2+} reduces the inhibitory effect of Mg^{2+}. The Mg^{2+} adsorption rate is determined by the $(a_{Mg})/(a_{Ca})$ ratio. An increase in a_{Ca} facilitates the growth of HAP crystals with less disturbance of the amelogenin and Mg.

Enamel fluid contains about 0.8 mM Mg^{2+} and 10 mM CO_3^{2-}. The Mg^{2+} inhibits the growth of HAP [79, 83], and the degree of inhibition is synergistically increased by CO_3^{2-} [83, 135]. Nevertheless, enamel crystal has good crystallinity. This can be ascribed in part to the cooperative regulation by amelogenin, Ca^{2+}, and Mg^{2+}, maintaining an a_{Ca} level suitable for growing HAP with good quality.

5.5 Evolution and Adopted Mineral Phase in Hard Tissue

In the evolution of animals, *Lingula unguis* (Brachiopoda, Inarticulata) appeared some 500 million years ago in the Ordovician period as an ancestor of animals with hard tissue [141]. *Lingula* still exists and is known as a living fossil. It has a pair of shells that cover its soft body like a bivalve. The shell is composed of apatite and β-chitin [142] instead of the typical $CaCO_3$ composition of Articulata (Brachiopoda) and Mollusca shells. Not only did species with an apatite shell appear prior to those

with a $CaCO_3$ shell, the *c*-axis of the HAP and the fiber axis of the β-chitin are parallel to each other [143, 144]. This orientation relationship between the HAP and organic matrix component indicates that a mechanism that organizes mineral crystal growth is inherent in animals with hard tissues.

HAP in a dense fraction (2.5–2.7 $g\,cm^{-3}$) of *Lingula* shell contains CO_3^{2-} (2.5 ± 0.2 wt%), F^- (2.0 ± 0.04 wt%), and Mg^{2+} (0.98 ± 0.01 wt%) with Cl^- as a minor component and structural water. Hydroxyl was not detected by FTIR analysis. *Lingula* shell HAP was identified as CO_3, F, Cl-Ap [145]. TEM [146] and SAXS [147] studies of the shell demonstrated that mineral granules (about 50 nm in diameter) were distributed in the marginal part of the shell, i.e., the newly formed part. After calcination at 1,000 °C, *Lingula* shell HAP produced β-TCP (about 30%) along with HAP with improved crystallinity. Since ACP transforms into β-TCP after being calcined [148], the existence of ACP in *Lingula* shell HAP is highly probable.

Chimaera phantasma (Holocephali), a relative of the shark, has a unique dental tissue "tooth plate" instead of sharp, marginal teeth like a shark. The tooth plate is composed of pleromin and osteodentin. The mineral phase of pleromin is whitlockite [149], and that of osteodentin is HAP. The whitlockite crystallizes in an oval shape, has high crystallinity, and deposits without orientation. *Chimaera* is a living fossil that appeared some 400 million years ago in the Devonian period. The lungfish (*Protopterus*) also has tooth plates; however, the mineral phase is HAP [150]. Thus, only *Chimaera phantasma* has dental tissue composed of whitlockite.

Recently, Bentov et al. [151] reported coexistence of calcium carbonates and calcium phosphate in the mandibles of a freshwater crayfish (the arthropod *Cherax quadricarinatus*): Amorphous calcium carbonate (ACC) and ACP located in the base of the mandible, F-Ap crystals covered the amorphose minerals, forming an enamel-like coating, and calcite located in the incisor. The use of both carbonates and phosphates as component of a functioning hard tissue was found, probably, for the first time in an evolution of biominerals.

"What determines the phase and organization of mineral in hard tissues" is an unanswered question. The higher level organizing system is thought to control the cells so that they provide a medium in which appropriate mineral can form. Recent advances in gene analysis and cloning techniques have made it possible to investigate the evolution of enamel proteins. The amino acid sequences of amelogenin have a striking level of homology among species [152, 153]. Further progress in this field could help answer the question above.

5.6 Concluding Remarks

Nucleation and growth of enamel HAP crystal proceed in an enamel matrix, which acts as a functional medium that changes the composition continuously, thereby providing an optimal environment for crystal formation. The formation process is determined by the local environment, which is determined by the tissue-specific cells. Analyses of developing enamel HAP crystal and of the components and

properties of the enamel matrix, along with in vitro evidence provided by advanced technologies, have been improving our understanding of tooth enamel formation. Further in vitro studies should enable us to better explain the mechanisms and fine-tune the formation scenario and new findings, like the coexistence of phosphates and carbonates in the crayfish mandibles, might require reconstruction of a phylogenic perspective of biominerals.

References

1. Nanci, A.: TenCate's oral histology: histology development, & function. Chapter 7, pp. 138–179. Mosby Inc., (2003)
2. Watson, M.L.: The extracellular nature of enamel in the rat. J Biophys Biochem Cytol **23**, 447–497 (1960)
3. Fukae, M., Shimizu, M.: Studies on the proteins of developing bovine enamel. Arch Oral Biol **19**, 381–386 (1974)
4. Glimcher, M.J., Mechanis, G.L., Friberg, U.A.: The amino acid composition of the organic matrix and the neutral soluble and acid soluble components of embrionic bovine enamel. Biochem J **93**, 198–202 (1964)
5. Robinson, C., Hiller, C.R., Weatherell, J.A.: Uptake of ^{32}P-labelled phosphate into developing rat incisor enamel. Calcf. Tissue. Res. **15**, 143–152 (1974)
6. Bawden, J.W., Merritt, D.H., Deaton, T.G.: In vitro study of calcium-45 and phosphorus-32 uptake in developing rat molar enamel using quantitative methods. Arch Oral Biol **26**, 477–482 (1981)
7. Takano, Y., Crenshaw, M.A., Bawden, J.W., Hammarstrom, L., Lindskog, S.: The Visualization of the patterns of ameloblast modulation by the glyoxal bis(2-hydroxyanil) staining method. J Dent Res **61**, 1580–1586 (1982)
8. Takano, Y., Crenshaw, M.A., Reith, E.J.: Correlarion of ^{45}Ca incorporation with maturation ameloblast morphology in the rat incisor. Calcif Tissue Int **34**, 211–213 (1982)
9. Kawamoto, T., Shimidzu, M.: Changes in the mode of calcium and phosphate transport during rat incisal enamel formation. Calcif Tissue Int **46**, 406–414 (1990)
10. Kawamoto, T., Shimidzu, M.: Changes of the ratio of calcium to phosphate transported into the mineralizing enamel, dentin, and bone. Jpn J Oral Biol **36**, 365–382 (1994)
11. Deakins, M.: Changes in the ash, water, and organic content of pig enamel during calcification. J Dent Res **21**, 429–435 (1942)
12. Robinson, C., Briggs, H.D., Atkinson, P.J., Weatherell, J.A.: Matrix and mineral changes in developing enamel. J Dent Res **58**, 871–880 (1984)
13. Weidmann, S.M., Weatherell, J.A., Hamm, S.: Variations of enamel density in sections of human teeth. Arch Oral Biol **12**, 85–97 (1967)
14. Eastoe, J.E.: The amino acid composition of proteins from the oral tissue-II. The matrix proteins in dentine and enamel from developing human deciduous teeth. Arch Oral Biol **8**, 633–652 (1963)
15. Fincham, A.G.: The amelogenin problem; A comparison of purified enamel matrix proteins. Calcif Tissue Int **26**, 65–73 (1979)
16. Takagi, T., Sasaki, S., Baba, T.: Complete amino acid sequence of amelogenin in developing bovine enamel. Biochem Biophys Res Commun **121**, 592–597 (1984)
17. Snead, M.L., Lau, E.C., Zeichner-David, M., Fincham, A.G., Woo, S.L.C., Slavkin, H.C.: DNA sequence for cloned cDNA for murine amelogenin reveal the amino acid sequence for enamel-specific protein. Biochem Biophys Res Commun **129**, 812–818 (1985)
18. Simmer, J.P., Lau, E.C., Hu, C.C., Aoba, T., Lacey, M., Nelson, D., Zeichner-David, M., Snead, M.L., Slavkin, H.C., Fincham, A.G.: Isolation and characterization of a mouse amelogenin expressed in *Escherichia coli*. Calcif Tissue Int **54**, 312–319 (1994)

19. Tan, J., Leung, W., Moradian-Oldak, J., Zeichner-David, M., Fincham, A.G.: Quantitative analysis of amelogenin solubility. J Dent Res **77**, 1388–1396 (1998)
20. Fincham, A.G., Moradian-Oldak, J., Simmer, J.P., Sarte, P.E., Lau, E.C., Diekwisch, T.G.H., Slavkin, H.C.: Self-assembly of a recombinant amelogenin protein generates supra-molecule structures. J Struct Biol **112**, 103–109 (1994)
21. Moradian-Oldak, J., Simmer, J.P., Lau, E.C., Sarte, P.E., Slavkin, H.C., Fincham, A.G.: Detection of monodisperse aggregates of a recombinant amelogenin by dynamic light scattering. Biopolymers **34**, 1339–1347 (1994)
22. Moradian-Oldak, J., Leung, W., Fincham, A.G.: Temperature and pH-dependent supramolecular self-assembly of amelogenin molecules: A dynamic light-scattering analysis. J Struct Biol **122**, 320–327 (1998)
23. Aoba, T., Fukae, M., Tanabe, T., Shimizu, M., Moreno, E.C.: Selective adsorption of porcine amelogenins onto hydroxyapatite and their Inhibitory activity on hydroxyapatite growth in supersaturated solutions. Calcif Tissue Int **41**, 281–289 (1987)
24. Moradian-Oldak, J., Leung, W., Tan, J., Fincham, A.G.: Interaction of amelogenin with hydroxyapatite crystals: An adherence effect through amelogenin molecular self-association. Bioploymers **46**, 225–238 (1998)
25. Ryu, O.H., Hu, C.C., Simmer, J.P.: Biochemical characterization of recombinant mouse amelogenin: protein quantitation, proton absorption, and relative affinity for enamel crystals. Connect Tissue Res **38**, 207–214 (1998)
26. Gibson, C.W., Golub, E., Abrams, W.R., Shen, G., Ding, W., Rosenbloom, J.: Bovine amelogenin message heterogeneity: alternative splicing and Y-chromosomal gene transcription. Biochemistry **31**, 8384–8388 (1992)
27. Simmer, J.P., Hu, C.C., Lau, E.C., Sarte, P.E., Moradian-Oldak, J., Slavkin, H.C., Fincham, A.G.: Alternative splicing of the mouse amelogenin primary RNA transcript. Calcif Tissue Int **55**, 302–310 (1994)
28. Hu, C.C., Yamakoshi, Y., Yamakoshi, F., Krebsbach, P.H., Simmer, J.P.: Proteomic and genetic of dental enamel. Cells Tissue Organ **181**, 219–231 (2005)
29. Brookers, S.J., Robinson, C., Kirkham, J., Bonass, W.A.: Biochemistry and molecular biology of amelogenin proteins of developing dental enamel. Arch Oral Biol **40**, 1–14 (1995)
30. Fincham, A.G., Moradian-Oldak, J., Simmer, J.P.: The structural biology of the developing dental enamel matrix. J Struct Biol **126**, 270–299 (1999)
31. Yanagisawa, T., Nylen, M.U., Termine, J.D.: Distribution of matrix components in hamster enamel. Electron microscopic study. J Dent Res **60**(A), 558 (1981)
32. Yamakoshi, Y.: Carbohydrate moieties of porcine 32 kDa enamelin. Calcif Tissue Int **56**, 323–330 (1995)
33. Termine, J.D., Belcourt, A.B., Christner, P.J., Conn, K.M., Nylen, M.U.: Properties of dissociatively extracted fetal tooth matrix proteins. 1. Principle molecular species in developing bovine enamel. J Biol Chem **255**, 9760–9768 (1980)
34. Tanabe, T., Aoba, T., Moreno, E.C., Fukae, M., Shimizu, M.: Properties of phosphrylated 32 kDa nonamelogenin proteins isolated from porcine secretory enamel. Calcif Tissue Int **46**, 205–215 (1990)
35. Deutsch, D., Palmon, A., Fisher, L., Termine, J.D., Young, M.: Sequencing of bovine enamelin ('Tuftelin'), A novel acidic enamel protein. J Biol Chem **266**, 16021–16028 (1991)
36. Fukae, M., Tanabe, T., Uchida, T., Yamakoshi, Y., Shimizu, M.: Enamelins in the newly formed bovine enamel. Calcif Tissue Int **53**, 257–261 (1993)
37. Hu, C.C., Fukae, M., Uchida, T., Qian, Q., Zhang, C.H., Ryu, O.H., Tanabe, T., Yamakoshi, Y., Murakami, C., Dohi, N., Shimizu, M., Simmer, J.P.: Cloning, and characterization of porcine enamelin mRNAs. J Dent Res **76**, 1720–1729 (1997)
38. Yamakoshi, Y., Pinheiro, F.H., Tanabe, T., Fukae, M., Shimizu, M.: Sites of asparagine-linked oligosaccharides in porcine 32 kDa enamelin. Connect Tissue Res **39**, 39–46 (1998)
39. Fukae, M., Tanabe, T.: Non-amelogenin components of porcine enamel in the protein fraction from enamel crystals. Calcif Tissue Int **40**, 286–293 (1987)

40. Uchida, T., Fukae, M., Tanabe, T., Yamakoshi, Y., Satoda, T., Murakami, C., Takahashi, O., Shimizu, M.: Immnolchemical and immnocytochemical study of a 15 kDa non-amelogenin and related proteins in the porcine immature enamel: Proposal of a new group of enamel proteins sheath proteins. Biomed Res **16**, 131–140 (1995)
41. Hu, C.C., Fukae, M., Uchida, T., Qian, Q., Zhang, C.H., Ryu, O.H., Tanabe, T., Yamakoshi, Y., Murakami, C., Dohi, N., Shimizu, M., Simmer, J.P. : Sheathlin cloning, cDNA/polypeptide sequences, and immunolocalization of porcine enamel sheath proteins. J Dent Res **76**, 648–657 (1997)
42. Fearnhead, R.W.: Mineralization of rat enamel. Nature **188**, 509–600 (1960)
43. Reith, E.J.: The early stage of amelogenesis as observed in molar teeth of young rats. J Ultrastruct Res **17**, 503–526 (1967)
44. Beniash, E., Metzler, R.A., Lam, R.S.K., Gilbert, P.U.P.A.: Transient amorphous calcium phosphate in forming enamel. J Struct Biol **166**, 133–143 (2009)
45. Brown, W.E., Lehr, J.R., Smith, J.P., Frazier, A.W.: Octacalcium phosphate and hydroxyapatite. Nature **196**, 1048–1055 (1962)
46. Brown, W.E.: Crystal Growth of bone mineral. Clin. Orthop. **44**, 205–220 (1966)
47. Cuisinier, F.J.G., Steuer, P., Senger, B., Vogel, J.C., Frank, R.M.: Human amelogenesis—high resolution electron microscopy of nanometer sized particles. Cell Tissue Res **273**, 175–182 (1993)
48. Bodier-Houlle, P., Steuer, P., Meyer, J.M., Bigeard, L., Cuisinier, F.J.G.: High resolution electron microscopic study of the relationship between human enamel and dentin crystals at the dentimo-enamel junction. Cell Tissue Res **301**, 389–395 (2000)
49. Rönnholm, E.: The amelogenesis of human teeth as revealed by electron microscopy. (II) The development of the enamel crystallites. J Ultrastruct Res **6**, 249–303 (1962)
50. Nylen, M.U., Eanes, E.D., Omnell, K.A.: Crystal growth in rat enamel. J Cell Biol **18**, 109–123 (1963)
51. Travis, D.F., Glimcher, M.J.: The structure and organization of, and the relationship between the organic matrix and the inorganic crystals of embryonic bovine enamel. J Cell Biol **23**, 447–497 (1964)
52. Weiss, M.P., Vogel, J.C., Frank, R.M.: Enamel crystallite growth: width and thickness study related to the possible presence of octacalcium phosphate during amelogenesis. J Ultrastruct Res **76**, 286–292 (1981)
53. Daculci, G., Menanteau, J., Kerevel, L.M., Mitre, D.: Enamel crystals: size Shape, length and growing process; High resolution TEM and biochemical study. In: Fearnhead, R.W., Suga, S. (eds.) Tooth Enamel IV, pp. 14–23. Elsevier Sci. Pub, Amsterdam (1984)
54. Kerebel, B., Daculsi, G., Kerebel, L.M.: Ultrastructural studies of enamel crystallites. J Dent Res **58**, 844–850 (1979)
55. Nylen, M.U.: Matrix-mineral relationships—a morphologist's viewpoint. J Dent Res **58**(B), 922–926 (1979)
56. Pain, M.L., Snead, M.L.: Protein interactions during assembly of the enamel organic extracellular matrix. J Bone Miner Res **12**, 221–227 (1997)
57. Lakshminarayanan, R., Fan, D., Du, C., Moradian-Oldak, J.: The role of secondary structre in the entropically driven amelogenin self-assembly. Biophys J **93**, 3664–3674 (2007)
58. Wen, H.B., Moradian-Oldak, J., Leung, W., Bringas Jr., P., Fincham, A.G.: Microstructures of an amelogenin gel matrix. J Struct Biol **126**, 42–51 (1999)
59. Wiedemann-Bidlack, F.B., Beniash, E., Yamakoshi, Y., Simmer, J.P., Margolis, H.C.: PH triggered self-assembly of native and recombinant amelogenins under physiological pH and temperature. J Struct Biol **160**, 57–69 (2007)
60. Moradian-Oldak, J., Du, C., Falini, G.: On the formation of amelogenin Microribbons. Eur J Oral Sci **114**, 289–296 (2006)
61. Fincham, A.G., Moradian-Oldak, J., Diekwisch, T.G.H., Lyaruu, D.M., Wright, J.T., Bringas Jr., P., Slavkin, H.C.: Evidence for amelogenin "nanospheres" as functional components of secretory-stage enamel matrix. J Struct Biol **115**, 50–59 (1995)

62. Moradian-Oldak, J., Lau, E.C., Diekwisch, T.G.H., Slavkin, H.C., Fincham, A.G.: A review of the aggregation properties of a recombinant amelogenin. Connect Tissue Res **32**, 125–130 (1995)
63. Margoris, H.C., Beniash, E., Fowler, E.C.: Role of macromolecular assembly of enamel matrix proteins in enamel formation. J Dent Res **85**, 775–793 (2006)
64. Fukae, M., Yamamoto, R., Karakido, T., Shimoda, S., Tanabe, T.: Micelle structure of amelogenin in porcine secretory enamel. J Dent Res **86**(8), 758–763 (2007)
65. Bartlett, J.D., Simmer, J.P.: Proteinases in developing dental enamel. Crit Rev Oral Biol Med **10**, 425–441 (1999)
66. Simmer, J.P., Fukae, M., Tanabe, T., Ymakoshi, Y., Uchida, T., Xue, J.: Purification, characterization, and cloning of enamel matrix serine protease 1. J Dent Res **77**, 377–386 (1998)
67. Goto, Y., Kogure, E., Takagi, T., Aimoto, S., Aoba, T.: Molecular conformation of porcine amelogenin in solution: three folding units at the N-terminal, central, and C-terminal regions. J Biochem **113**, 55–60 (1993)
68. Matsushima, N., Izumi, Y., Aoba, T.: Small-angle X-Ray scattering and computer-Aided molecular modeling studies of 20 kDa fragment of porcine amelogenin: Does amelogenin adopt an elongated bundle structure? J Biochem **123**, 150–156 (1998)
69. Aoba, T., Moreno, E.C.: The enamel fluid in the early secretory stage of porcine amelogenesis: chemical composition and saturation with respect to enamel mineral. Calcif Tissue Int **41**, 86–94 (1987)
70. Amano, T., Sato, K., Aoba, T.: Soluble constituents in the fluid environment of pig and rat developing enamel and their relevance to the regulation of mineralization. Jpn J Oral Biol **43**, 257–267 (2001)
71. Sasaki, S., Takagi, T., Suzuki, M.: Cyclic changes in pH in bovine developing enamel as sequential bands. Arch Oral Biol **36**, 227–231 (1991)
72. Moreno, E.C., Aoba, T.: Comparative solubility study of human dental enamel, dentin, and hydroxyapatite. Calcif Tissue Int **49**, 6–13 (1991)
73. McConnel, D.: Recent advance in the investigation of the crystal chemistry of dental enamel. Arch Oral Biol **3**, 28–34 (1960)
74. Aoba, T., Moreno, E.C.: Changes in the nature and composition of enamel mineral during porcine amelogenesis. Calcif Tissue Int **47**, 356–364 (1990)
75. Aoba, T., Moreno, E.C.: Changes in the solubility of enamel mineral at various stages of porcine amelogenesis. Calcif Tissue Int **50**, 266–272 (1992)
76. Shimoda, S., Aoba, T., Moreno, E.C.: Acid-phosphate contents in porcine enamel mineral at various stages of amelogenesis. J Dent Res **70**, 1516–1523 (1991)
77. Aoba, T., Sato, K.: Mechanism of developmental enamel mineralization: enamel fluid, crystals, and organic matrix. In Tooth Ename, (Association for Comparative Biology of Tooth Enamel), pp.67–81. Wakaba Pub. Inc., Japan (2009)
78. Moreno, E.C., Kresak, M., Zahradnik, R.T.: Fluoridated hydroxyapatite solubility and caries formation. Nature **247**, 64–65 (1974)
79. Brown, W.E., Mathew, M., Tung, M.S.: Crystal chemistry of octacalcium phosphate. In: Pamplin, B.R. (ed.) Progress in crystal growth and characterization, vol. 4, pp. 59–87. Pergamon Press Ltd., Great Britain (1981)
80. LeGeroe, R.Z.: Calcium phosphate in oral biology and medicine. Karger, Baskel (1991)
81. Elliott, J.C.: Structure and chemistry of the apatites and other calcium orthophosphates, vol. 18. Studies in inorganic chemistry, Elsevier, London (1994)
82. Chickerur, N.S., Tung, M.S., Brown, W.E.: A mechanism for incorporation of carbonate into apatite. Calcif Tissue Int **32**, 55–62 (1980)
83. LeGeroe, R.Z.: Apatites in biological systems. In: Pamplin, B.R. (ed.) Progress in crystal growth and characterization, vol. 4, pp. 1–45. Pergamon Press Ltd., Great Britain (1981)
84. Shimoda, S., Aoba, T., Moreno, E.C., Miake, Y.: Effect of solution composition on morphological and structural feature of carbonated calcium apatites. J Dent Res **69**, 1731–1740 (1990)

85. Posner, A.S., Perloff, A., Diorio, A.F.: Refinement of the hydroxyapatite structure. Acta Cryst **11**, 308–309 (1958)
86. Kay, M.I., Young, R.A., Posner, A.S.: Crystal structure of hydroxyapatite. Nature **204**, 1050–1052 (1964)
87. Young, R.A., Elliott, J.C.: Atomic-scale bases for several properties of apatites. Arch Oral Biol **11**, 699–707 (1966)
88. Young, R.A., Mackie, P.E.: Crystallography of human tooth enamel: initial structure refinement. Mater Res Bull **15**, 17–29 (1980)
89. Young, R.A.: Implication of atomic substitutions and other structural details in apatites. J Dent Res **53**, 193–203 (1974)
90. Hagen, A.R.: Structural features of biologicaly involved phosphates. Acta Odontol Scand **31**, 149–173 (1973)
91. Arsenault, A.L., Robinson, B.W.: The Dentino-enamel junction: a structural and microanalytical study of early mineralization. Calcif Tissue Int **45**, 111–121 (1989)
92. Diekwisch, T.G.H., Berman, B.J., Gentner, S., Slavkin, H.C.: Initial enamel crystals are not spatially associated with mineralized dentin. Cell Tissue Res **279**, 149–167 (1995)
93. Beniash, E., Simmer, J.P., Margoris, H.C.: The Effect of recombinant mouse amelogeneses nn the formation and organization of hydroxyapatite crystals in vitro. J Struct Biol **149**, 182–190 (2005)
94. Tao, J., Pan, H., Zeng, Y., Xu, X., Tang, R.: Roles of Amorphous calcium phosphate and biological additives in the assembly of hydroxyapatite nanoparticles. J Phys Chem **111**, 13410–13418 (2007)
95. Wang, L., Guan, X., Chang, D., Moradian-Oldak, J., Nancollas, G.H.: Amelogenin promotes the formation of elongated apatite microstructures in a controlled crystallization system. J Phys Chem **111**, 6398–6404 (2007)
96. Yang, X., Wang, L., Qin, Y., Sun, Z., Henneman, Z.J., Moradian-Oldak, J., Nancollas, G.H.: How amelogenin orchestrates the organization of hierarchical elongated microstructures of apatite. J Phys Chem **114**(6), 22293–22300 (2010)
97. Shaw, W.J., Campbell, A.A., Pain, M., Snead, M.L.: The COOH terminus of the amelogenin, LRAP, is oriented next to hydroxyapatite surface. J Biol Chem **279**, 40263–40266 (2004)
98. Tarasevich, B.J., Howard, C.J., Larson, J.L., Snead, M.L., Simmer, J.P., Pain, M., Shaw, W.J.: The nucleation and growth of calcium phosphate by amelogenin. J Cryst Growth **304**, 407–415 (2007)
99. Kirkham, J., Zhang, J., Brookes, S.J., Shore, R.C., Ryu, O.H., Wood, S.R., Smith, D.A., Wallwork, M.L., Robinson, C.: Evidence for charge domains on developing enamel crystal surfaces. J Dent Res **79**, 1943–1947 (2000)
100. Bouropoulos, N., Moradian-Oldak, J.: Induction of apatite by the cooperative effect of amelogenin and 32 kDa enamelin. J Dent Res **83**, 278–282 (2004)
101. Fan, D., Lakshminarayanan, R., Moradian-Oldak, J.: The 32 kDa enamelin undergoes conformational transitions upon calcium binding. J Struct Biol **163**, 109–115 (2008)
102. Fan, D., Chan, D., Sun, Z., Lakshminarayanan, R., Moradian-Oldak, J.: In vitro study on the interaction between the 32 kDa enamelin and amelogenin. J Struct Biol **166**, 88–94 (2009)
103. Iijima, M., Fan, D., Bromly, K. M., Sun, Z., Moradian-Oldak, J.: The 32 kDa enamelin undergoes conformational transitions upon calcium binding. Crystal Growth. Design, (under review). (2010)
104. Combes, C., Rey, C.: Amorphous calcium phosphates synthesis, properties and uses in biomaterials. Acta Biomaterialia. **6**(9), 3362–3378 (2010)
105. Eanes, D.E.: Amorphous calcium phosphate. In: Chow, L.C., Eanes, E.D. (eds.) Octacalcium phosphate, vol. 18, pp. 130–147. Monograp. Oral Sci, Basel, Karger (2001)
106. Eanes, E.D., Posner, A.S.: Intermediate phases in the basic solution preparation of alkaline earth phosphates. Calcif Tissue Res **2**, 38–48 (1968)
107. Termin, J.D., Peckauskas, R.A., Ponser, A.S.: Calcium phosphate formation in vitro. II. Effects of environment on amorphous-crystalline transition. Arch. Biochem. Biophys. **140**, 318–325 (1970)

108. Kwack, S.Y., Wiedemann-Bidlack, F.B., Beniash, E., Yamakoshi, Y., Simmer, J.P., Litman, A., Margolis, H.C.: Role of 20 kDa amelogenin (P148) phosphorylation in calcium phosphate formation in vitro. J Biol Chem **284**(28), 18972–18979 (2009)
109. Robinson, C., Shore, R.C., Wood, S.R., Brookes, S.J., Smith, D.A.M., Wright, J.T., Connell, S., Kirlkham, J.: Subunit structures in hydroxyapatite crystal development in enamel: implication for amelogenesis imperfecta. Connect Tissue Res **44**, 65–71 (2003)
110. Tomson, M.B., Nancollas, G.H.: Mineralization kinetics: a constant composition approach. Science **200**, 1059–1060 (1978)
111. Onuma, K., Ito, A.: Cluster growth model for hydroxyapatite. Chem Mat **10**, 3346–3351 (1998)
112. Oyane, A., Onuma, K., Kokubo, T., Ito, A.: Clustering of calcium phosphate in the system $CaCl_2$-H_3PO_4-KCl-H_2O. J Phys Chem B **103**, 8230–8235 (1999)
113. Eanes, E.D., Gillssen, I.H., Posner, A.S.: Intermediate states in the precipitation of hydroxyapatite. Nature **208**, 365 (1965)
114. Termine, J.D., Eanes, E.D.: Comparative chemistry of amorphous and apatitic calcium phosphate preparations. Calcif Tissue Res **10**, 171–197 (1972)
115. Eanes, E.D., Meyer, J.L.: The Maturation of crystalline calcium phosphates in aqueous suspensions at physiologic pH. Calcif Tissue Res **23**, 259–269 (1977)
116. Eanes, E.D.: Crystal growth of mineral phases in skeletal tissues. In: Pamplin, B.R. (ed.) Progress in crystal growth and characterization, vol. 3, pp. 3–15. Pergamon Press Ltd, Great Britain (1981)
117. Eanes, E.D., Termine, J.D., Nylen, M.U.: An electron microscopic study of the formation of amorphous calcium phosphate and its transition to crystalline apatite. Calcif Tissue Res **12**, 143–158 (1973)
118. Meyer, J.L.: Phase transformation in the spontaneous precipitation of calcium phosphate. Croat Chem Acta **56**, 753–767 (1983)
119. Brown, W.E., Schroeder, L.W., Ferris, J.S.: Interlayering of crystalline octacalcium phosphate and hydroxyapatite. J Phys Chem **83**, 1385–1388 (1979)
120. Miake, Y., Shimoda, S., Fukae, M., Aoba, T.: Epitaxial overgrowth of apatite crystals on the thin-ribbon precursor at early stages of porcine enamel mineralization. Calcif Tissue Int **53**, 249–256 (1993)
121. Tohda, H., Yamada, M., Yamaguchi, Y., Yanagisawa, T.: High-resolution electron microscopical observations of initial enamel crystals. J Electron Microsc **1**, 97–101 (1997)
122. Arnord, S., Plate, U., Wiesmann, H.P., Stratmann, U., Kohl, H., Holing, H.J.: Quantitative analyses of the biomineralization of different hard tissue. J Microsc **202**, 488–494 (2001)
123. Arends, J., Davidson, C.L.: HPO_4 contents in enamel and artificial carious lesions. Calcif Tissue Res **18**, 65–79 (1975)
124. Crane, N.J., Popescu, V., Morris, M.D., Steenhuis, P., Ignelzi Jr., M.A.: Raman spectroscopic evidence for octacalcium phosphate and other transient mineral species deposited during intramembranous mineralization. Bone **39**, 434–442 (2006)
125. Nelson, D.G.A., Wood, G.J., Barry, J.C., Featherstone, J.D.B.: The structure of (100) defects in carbonated apatite crystallites: A high resolution electron microscopy study. Ultramicroscopy **19**, 253–266 (1986)
126. Nakahara, H., Kakei, M.: Central dark line and carbonic anhydrase: Problems relating to crystal nucleation in enamel. In: Fearnhead, R. W., Suga, S. (eds.) Tooth Enamel IV. pp. 42–46, 82. Elsevier Sci. Pub., Amsterdam (1984)
127. Cuisinier, F.J.G., Steuer, P., Senger, B., Vogel, J.C., Frank, R.M.: Human amelogenesis I: High resolution electron microscopy study of ribbon-like crystals. Calcif Tissue Int **51**, 259–268 (1992)
128. Nelson, D.G.A., Barry, J.C.: High resolution electron microscopy of nonstichometric apatite crystals. Anat Rec **224**, 265–276 (1989)
129a. Iijima, M., Tohda, H., Moriwaki, Y.: Growth and structure of lamellar mixed crystals of octacalcium phosphate and apatite in a model system of enamel formation. J Cryst Growth **116**, 319–326 (1992)

129b. Iijima, M., Tohda, H., Suzuki H., Yanagisawa T., Moriwaki, Y.: Effect of F on apatite octacalcium phosphate intergrowth and morphology in a model system of tooth enamel formation. Calcif. Tiss. Int. **50**, 357–361 (1992)
130. Aoba, T., Miake, Y., Shimoda, S., Prostak, K., Moreno, E.C., Suga, S.: Dental apatites in vertebrates species: morphology and chemical properties. In: Nakahara, H., Suga, S. (eds.) Mechanisms and phylogeny of mineralization in biological systems, pp. 459–463. Springer-Verlag, Tokyo (1991)
131. Miake, Y., Aoba, T., Moreno, E.C., Shimoda, S., Prostak, K., Suga, S.: Ultrastructural studies on crystal growth of enameloid minerals in elasmobranch and teleost fish. Calcif Tissue Int **48**, 204–217 (1991)
132. Kakei, M., Sakae, T., Yoshikawa, M.: Electron microscopy of octacalcium phosphate in the dental calculus. J Electron Microsc **58**(6), 393–398 (2010)
133. Osborn, J.W.: The mechanism of prism formation in teeth: a hypothesis. Calcif Tissue Int **5**, 115–132 (1970)
134. Moriwaki, Y., Doi, Y., Kani, T., Aoba, T., Takahashi, J., Okazaki, M.: Synthesis of enamel-like apatite at physiological temperature and pH using ion-selective membranes. In: Suga, S. (ed.) Mechanism of tooth enamel formation, pp. 239–256. Quintessence, Tokyo (1983)
135. Iijima, M.: Formation of octacalcium phosphate in vitro. In: Chow, L.C., Eanes, E.D. (eds.) Octacalcium phosphate, vol. 18, pp. 17–49. Karger, Monograp. Oral Sci. (2001)
136. Hata, M., Moriwaki, Y., Doi, Y., Goto, T., Wakamatu, N., Kamemizu, H.: Oriented growth of octacalcium phosphate on cation selective membrane (in Japanese). Jpn J Crystal Growth **12**, 91–99 (1985)
137. Aoba, T., Fejerskov, O.: Dental fluorosis: chemistry and biology. Crit Rev Oral Biol Med **13**(2), 155–170 (2002)
138. Iijima, M., Moriwaki, Y., Takgi, T., Moradian-Oldak, J.: Effects of bovine amelogenins on the crystal morphology of octacalcium phosphae in a model system of tooth enamel formation. J Cryst Growths **222**, 615–626 (2001)
139. Iijima, M., Moradian-Oldak, J.: Control of octacalcium phosphae and apatite growth by amelogenin matrices. J Mater Chem **14**, 2189–2199 (2004)
140. Iijima, M., Moradian-Oldak, J.: Control of apatite crystal growth in a fluoride containing amelogenin-rich matrix. Biomaterials **26**, 1595–1603 (2005)
141. Chapman, F.: Notes on shell-structure in the genus *Lingula*, Recent and Fossil. J R Micro Soc **5**, 28–31 (1914)
142. Klement, R.: Die anorganshe skeletsubstantz. Ihre zusammensetzung, naturlichs unt kunstliche bildung. Naturewissenshaften **26**, 145–152 (1938)
143. Kelly, P. G., Oliver, P. T. P., Pautard, F. G. E.: The shell of Lingula unguis. Proc. 2nd. Eur. Symp. Calcif. Tissue. 337-345. (1965)
144. Iijima, M., Moriwaki, Y.: Orientation of apatite and organic matrix in *Lingula unguis* shell. Calcif Tissue Int **47**, 237–242 (1990)
145. Iijima, M., Kamemizu, H., Wakamatu, N., Goto, T., Moriwaki, Y.: Thermal decomposition of Lingula shell apatite. Calcif Tissue Int **49**, 128–133 (1991)
146. Iwata, K.: Ultrastructure and calcification of the shells in inarticulate Brachiopods. I. Ultrastructure of Lingula unguis (LINNAEUS). J Geol Soc Jpn **87**, 405–415 (1981)
147. Iijima, M., Moriwaki, Y., Gyotoku, T., Hayashi, K., Imura, S.: Small angle X-ray scattering study of Lingula unguis shell. Jpn J Oral Biolt **31**, 308–316 (1989)
148. Eanes, E.D.: Thermodynamical studies on amorphous calcium phosphate. Calcif Tissue Res **5**, 133–145 (1970)
149. Ishiyama, M., Sasagawa, I., Akai, J.: The inorganic content of pleromin in tooth plates of the living Holocephalan consists of a crystalline calcium phosphate known as ß-$Ca_3(PO_4)_2$ (whitlockite). Arch Histol Jpn **47**, 89–94 (1984)
150. Ishiyama, M., Teraki, Y.: The fine structure and formation of hypermineralized petrodentine in tooth plate of extant Lungfish. Arch Histol Cytol **53**, 307–321 (1990)

151. Bentov, S., Zaslansky, P., Sawalmih, A.A., Masic, A., Fratzl, P., Sagi, A., Berman, A., Aichmayer, B.: Enamel-like apatite crown covering amorphous mineral in a crayfish mandible. Nat Commun **3**, 839 (2012). doi:10.1038/ncomms1839
152. Bonass, W.A., Robinson, P.A., Kirkham, J., Shore, R.C., Robinson, C.: Molecular cloning and DNA sequence of Rat amelogenin and a comparative analysis of mammalian amelogenin protein sequence divergence. Biochem Biophys Res Commun **198**, 755–763 (1994)
153. Toyosawa, S., O'hUign, C., Figueroa, F., Tichy, H., Klein, J.: Identification and characterization of amelogenin genes in monotremes, reptiles and amphibians. Proc Natl Acad Sci U S A **95**, 13056–13061 (1998)